Compensated Surface Plasmon Resonance Sensor for Long-Term Monitoring Applications

Compensated Surface Plasmon Resonance Sensor for Long-Term Monitoring Applications

Carmelo Fallauto, Yu Liu, Guido Perrone, *Member, IEEE*, and Alberto Vallan, *Senior Member, IEEE*

***Abstract*— This paper presents an optical sensor capable of detecting small changes in the concentration of chemicals by exploiting the surface plasmon resonance principle. A two sensing area layout allows implementing a differential configuration to compensate the perturbations—such as mechanical instabilities and temperature fluctuations—that greatly impair the accuracy especially during long-term monitoring applications. The proposed solution can be easily implemented in different geometries, including optical fibers. An analysis of the impact of unwanted changes in the measurement setup is provided and an example of a compensation procedure applied to angular misalignments is given. Experimental validation and analysis of uncertainty sources affecting the proposed compensation procedure are reported.**

***Index Terms*— Chemical fiber optic sensors, evanescent wave sensing, fiber optic sensors, surface plasmon resonance (SPR).**

I. Introduction

OPTICAL means for the detection of chemicals and biochemicals are gaining an increasing popularity because of their very high sensitivity combined with adaptability to harsh environments, which is given by their intrinsic properties such as impossibility to start fires or explosions, immunity from electromagnetic interference, absence of electrocution risks, and resistance to corrosion. Hence, many optical sensing principles have been proposed in the recent years, but the most promising are those based on the interaction between the evanescent field tails of a light beam and the substance whose concentration has to be measured [1], [2]. In particular, one of the most relevant sensing techniques is the surface plasmon resonance (SPR), which is able to detect part-per-billion changes in the concentration of a chemical (analyte), in real time, and without the need of specific labels.

SPR sensors exploit the excitation of plasma waves at a metal–dielectric interface through an evanescent wave; then they relate the variation of the propagation constants of these plasma waves with the changes in the concentration of the analyte [3], [4].

SPR-based devices are mainly implemented using discrete optical components (usually, the sensing area is made by the hypotenuse of a glass prism with a gold coating), although the trend is to move toward the development of fiber or integrated optical devices to take advantage of their compactness and mechanical stability.

In these cases, the metal layer is deposited in close proximity of the waveguide core, after partial or total removal of the cladding layer, and the excitation of the surface plasma wave is through the evanescent field tails of the guided modes.

As for the fibers, glass fibers similar to those employed in optical communications are used today [5], [6], but there is a growing interest to transfer the results to plastic optical fibers (POFs) because they would ease the fabrication of low cost, hence disposable, devices [7], [8]. Indeed, POF are characterized by a large core made of polymethyl methacrylate surrounded by a thin cladding made of fluorinated polymers, and have a very high numerical aperture, so that coupling and handling are simplified. Moreover, since removing the cladding is much easier for POF than for glass fibers [9], the fabrication of the sensors is simplified, with a further cost reduction. POF, however, suffer from quite a large variability with environmental conditions and ageing, so proper compensation techniques must be developed to allow their practical use. More in general, compensations are necessary to allow maintaining the excellent performance of SPR sensors in long-term monitoring applications. Actually, these sensors typically detect a change in the composition of the analyte through a variation of the received power at a specific wavelength and therefore, being essentially of the intensiometric type, suffer from all their drawbacks in terms of sensitivity to ageing, to perturbations from the mechanical setup, or to drifts in the electronic circuits. In other words, while resolution down to 10^{-7} refractive index units (RIUs) or better have already been demonstrated [2], [10], this performance can be easily spoiled by parasitic effects, especially when glass-based devices are replaced with plastic fibers to lower the overall costs.

In [11] and [12], the authors have proposed a preliminary version of a differential SPR-based sensor specifically designed for permanent monitoring, mainly in the areas of environment and safety; in this paper, the analysis of the sensor is extended and its performance are assessed through several experiments, carried out in different working conditions. Unlike some other differential configurations applied to SPR sensors [13], [14], the proposed compensated sensor can be easily implemented both in prism- and in waveguide-based setups; although in the following, it is mainly discussed with reference to a prism configuration because for that case it is easier to induce mechanical instabilities and thus demonstrate the compensation effectiveness.

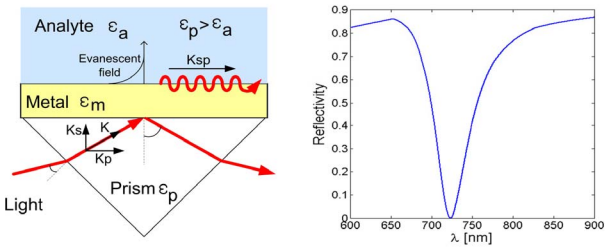

Fig. 1. SPR sensor typical implementation: Kretschmann prism configuration (left) and an example of the reflected power versus wavelength for a p-polarized beam at a given incident angle (right).

The remaining of this paper is organized as follows. In Section II, the SPR working principle is revised and the possible causes of uncertainties are highlighted; Then, in Section III, the compensation approach is introduced. Section IV provides an experimental validation of the compensation technique and, finally, Section V draws the conclusion.

II. SPR Sensor Working Principle and Origin of Instabilites

The excitation of a wave by coupling with another beam requires matching the wave vectors of incident and excited waves; in the case of surface plasmon waves (SPWs) at a metal–dielectric interface, this implies that the incident wave must be of the evanescent type. The simplest implementation of such excitation is the configuration that uses a prism under total internal reflection with a thin-metal layer deposited on the hypotenuse, as shown in the left side of Fig. 1.

Incident light is totally reflected at the prism–metal interface, except for the p-polarized components with wave vector satisfying the matching condition with SPW; for suitable metal thickness, this result in a notch-like response with the dip position that is strongly dependent on the refractive index of the chemical in contact with the metal layer (i.e., the analyte). Therefore, changes in the analyte composition imply variations in the refractive index that is then evaluated by measuring the shift of the notch position. Sensor interrogation can be practically implemented either using a broadband source at a fixed incident angle (wavelength interrogation) or a monochromatic source emitting a broad angular spectrum (angular interrogation) [15]. An example of the reflected power in the case of wavelength interrogation is shown in the right side of Fig. 1 for a specific combination of prism refractive index, metal layer material and thickness, incident angle, and analyte.

Despite its simplicity, this sensor configuration is able to detect refractive index changes better than 10^{-6} RIU; similar considerations apply also for the optical fiber configuration [2].

However, it is evident that any change in the source beam characteristics (e.g., due to drifts or misalignments), or in the prism and metal refractive indexes (e.g., due to temperature), is undistinguishable from actual variations in the analyte refractive index, and thus in its composition. This clearly poses severe limitations, especially in long-term monitoring applications. The effects of perturbations in the sensing setup are analyzed in this paper through both the simulations and experiments.

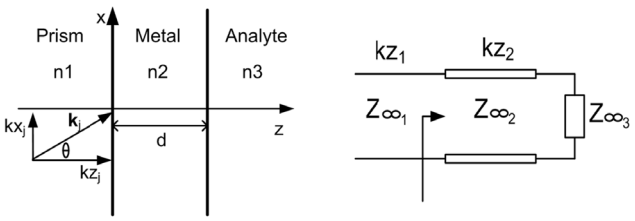

Fig. 2. Multilayer model of the prism-based sensor (left) and its equivalent in terms of transmission lines for each incident plane wave component.

As for the simulations, a model based on the equivalence between the cascade of transmission lines and multilayered media, such as those deposited on the prism or fiber surface to form the sensing areas, has been developed (Fig. 2).

According to this approach, for each plane wave component of the incident field, each layer can be substituted by a transmission line with characteristic impedance $Z_{\infty i,j}$ given by

$$Z_{\infty i,j}|^s = \frac{\omega\mu_i}{k_{z\ i,j}}$$

$$Z_{\infty i,j}|^p = \frac{k_{zi,j}}{\omega\varepsilon_i}$$

where the first relation holds for s-polarized waves and the second for p-polarized waves, $k_{zi,j}$ is the propagation constant of the jth plane wave component of the incident field in the ith medium, ω is the pulsation, and μ_i and ε_i are the ith layer magnetic permeability and dielectric permittivity, respectively. The ratio of the light intensity after reflection at the sensing areas and the incident light, for a given incident angle and wavelength, is computed as the return loss in the equivalent transmission lines problem. The refractive index of the materials and its dependency with wavelength and temperature has been computed through Sellmeier-type equations with coefficients taken from [16]–[18] or [19]. Before being applied to study the sensor performance, the model has been validated by comparing the theoretical predictions and measurements in a reference case, as described in [12]. Then, simulations have been run to consider the variability of the experimental conditions, such as the uncertainty in the gold layer thickness, and the instabilities that can affect the experimental setup, such mechanical misalignments that change the incidence angle, or temperature variations that impact both on the material refractive index and dimensions. It has been found that temperature induced uncertainties can be expressed in terms of equivalent angular variations and vice versa. Hence, considering, for example, the wavelength interrogation approach with a prism setup, angular misalignments can be representative of temperature fluctuation induced uncertainties too, as discussed in [11]. Therefore, in the following, for simplicity in controlling the amount of induced perturbation, the focus will be on wavelength interrogation of a prism setup and all the sources of uncertainties will be converted into equivalent angular misalignment.

To highlight the impact of angular misalignments on these sensors, Fig. 3 shows an example in which a $\pm 0.2°$ angular deviation from the nominal value produces shifts in the position of the SPR of a water-based solution that are undistinguishable from changes in the analyte refractive index of

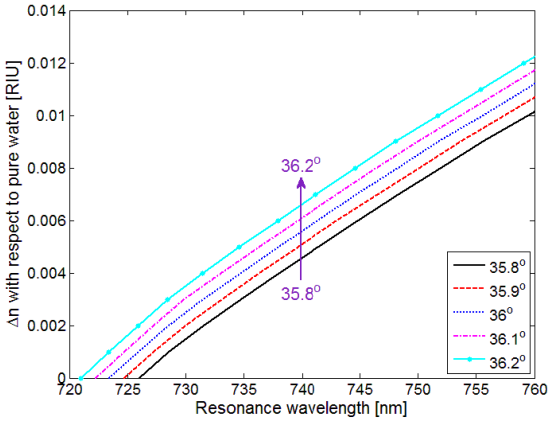

Fig. 3. Variation of the estimated refractive index of a water-based solution constituting the analyte, for wavelength interrogation and change in the incident air-prism angle.

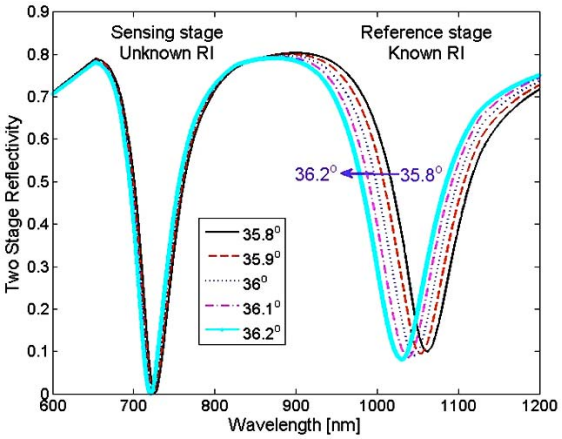

Fig. 5. Example of the effect of the incident beam angle change on the resonance position for water-based analyte and reference material having a refractive index of 0.045 larger than that of water.

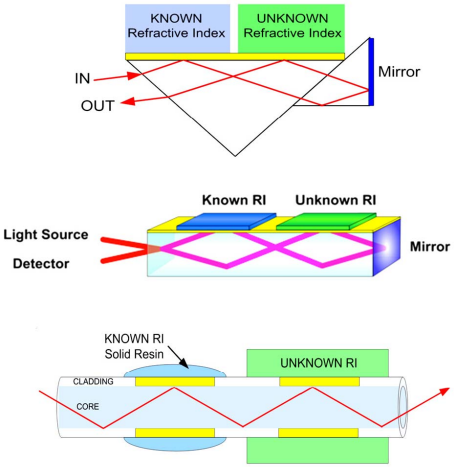

Fig. 4. Proposed differential sensor configuration: prism-based (above), waveguide (center), and all-fiber (below) implementations.

$\sim\pm\ 1{\cdot}10^{-3}$ RIU, a value well exceeding the typical resolution of SPR sensors. Similar effects can be obtained for temperature variation of ± 20 °C.

III. Compensated Sensor Configuration

The limitations in long-term monitoring can be mitigated using a differential configuration, like that shown in Fig. 4 in three different implementations for prism, waveguide, and fiber setups, respectively. Compared with other differential sensors in which the two sensing areas are in parallel configuration [13], the considered cascade approach simplifies a single all-fiber or waveguide realization and allows a more compact implementation with source and detectors on the same side even for the prism case.

The dual-stage compensated sensor working principle can be understood with reference to Fig. 4—top, in which a light beam excites the SPR at the first sensing area, then after some reflections it probes the second sensing area [20]. Additional sensing areas may be further added in cascade, provided their resonances are sufficiently separated to allow their respective detection without overlaps, but still within the interrogation system working range. A material with known refractive index, like a resin, covers one of the sensing areas, and it is used as a reference for drift compensation purposes. The transmission line based model can be easily extended to consider the cascade of sensing areas [12].

Fig. 5 shows an example of the impact of angular misalignment on the resonance positions when using the refractive index of water for the sensing stage and a value 0.045 RIU larger for the reference stage. As shown in the figure, a good choice for the reference material refractive index is to be slightly larger than that expected for the analyte to have a much larger sensitivity to angular misalignments in the reference rather than in the measuring stage, and thus to improve the effectiveness of the compensation procedure.

As already outlined, the curves in Fig. 5, although for angular misalignments, are representative also of temperature changes.

The readings from the reference stage are used to compensate those from the sensing stage with the procedure detailed in the following.

First, prior to the sensor fabrication, the dependence of the reference refractive index (low index resin in the setup considered in this paper) with the quantity representative of the perturbations (angular misalignments in this paper) is evaluated and a curve reporting the reference resonance position against the quantity representative of the perturbations is created, like the back solid curve in Fig. 6.

During the sensor normal operation both resonance positions are measured and, from the position of the reference resonance and with the help of the previously created charts, the equivalent incidence angle change is determined. Then, this angular correction is used to compute the new angle of incidence that is used in the theoretical model to estimate the analyte refractive index change. This is obtained by fitting the measured spectrum around the sensing resonance position using the simulations. The fitting between the measures and the simulations is carried out using a routine that implements the Nelder–Mead downhill simplex method with the analyte refractive index as the only unknown. In principle, an exact

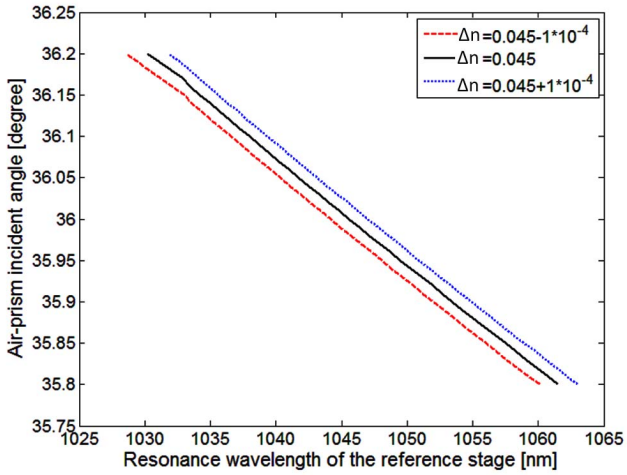

Fig. 6. Compensation function of the incident angle drift when the nominal value of reference analyte differs from that of the sensing area (pure water in this case) by $\Delta n = 0.045$. This figure also reports the uncertainty band due to a refractive index fluctuation of $\pm 1 \cdot 10^{-4}$ RIU.

compensation can be achieved, provided that the exact spectral position of the reference resonance is known and the refractive index of the reference material does not fluctuates. Being related to the experimental setup limitations, the effect of the resolution in the resonance wavelength determination is described in Section IV, where, moreover, examples of practical application of the compensation procedure are given.

As for the reference refractive index fluctuation, its impact is more difficult to analyze from an experimental point of view. Hence, to provide at least a qualitative estimation, from the model it is possible to infer that in the case considered in Fig. 6, a change during the measurement process on reference analyte by $\pm 1 \cdot 10^{-4}$ RIU from the nominal value (i.e., within the two lines around the central one in Fig. 6) produce an uncertainty of $\sim \pm 0.025°$ in angle estimation. This, in turn, produces an uncertainty in the measuring stage of $\pm 5 \cdot 10^{-5}$ RIU, after having applied the proposed angular compensation procedure. This result not only represents a relevant improvement with respect to the uncompensated case in Fig. 3, but also highlights the importance of the stability of the material chosen as reference over time (for instance, resins may change their properties with ageing, especially if exposed to UV light, but the analysis of these effects is beyond the scope of this paper).

IV. Experimental Results

To experimentally validate the compensation approach proposed in the previous section, the setup in Fig. 4—top has been realized by depositing (50 ± 4) nm of gold on the hypotenuse of a BK 7 prism through RF-assisted plasma sputtering. Then, part of the gold layer has been covered with a thick layer of UV-curable resin with nominal refractive index of 1.376 ± 0.005 at its resonance wavelength. Since in a typical drift of a few tenths of degrees, the relation between the resonance and incident angle is almost linear (Fig. 6), for an effective compensation it is not important to know exactly the refractive index of the reference stage, but it is only important that it remains constant over time.

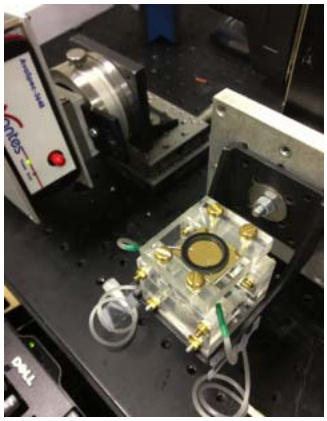

Fig. 7. Photography of the experimental setup.

The resin has been chosen to have a refractive index corresponding to a resonance position close to that of water because the sensing system under development is intended primarily for long-term monitoring of residual pesticides in water.

The prism has been mounted on a computer controlled precision rotary stage and a fluidic chamber has been realized to allow the injection of the analyte. Two different excitation conditions, namely broad wavelength range at fixed angle and change of angle at single wavelength, have been considered, but the results will be reported in the following for the former only. For this case, a constant-current driven halogen lamp followed by a linear polarizer has been used for the source, while the reflected light has been collected by spectrometer. The setup is shown in Fig. 7.

A preliminary measurement of the received light without the analyte is recorded to acquire the source spectrum that will be used to normalize the sensor spectral reading. The stability of the halogen lamp source has been evaluated by repeating the measure of the source spectrum several times at random intervals and no appreciable fluctuation as been found in the power distribution for at least 10 h.

During normal sensor operation, the analyte solution is injected into the chamber and one hundred measurements are acquired and averaged to reduce the noise. Having the goal in this paper of evaluating the compensation effectiveness only, pure distilled water is used as the unknown analyte in the next graphs. Furthermore, to highlight the role of the two sensing areas, measurements obtained by selectively exciting reference and sensing areas, respectively, have also been taken, as shown, for example, in Fig. 8. In particular, this figure reports the spectral response of the reference and sensing areas for angular misalignment intentionally induced in steps of 0.1° using a computer controlled precision rotation stage.

The curves in Fig. 8 are the equivalent of those in Fig. 5, except that the setup is working at a different beam incident angle to have the resonances positioned at wavelengths at which the source has higher intensity, and thus to operate in a more favorable signal-to-noise ratio.

To detect refractive index changes in the order of 10^{-6} RIU following the compensation procedure described in the previous section, it is necessary to track the shifts in

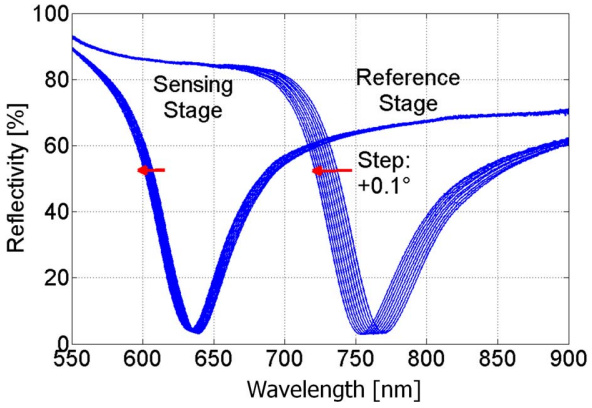

Fig. 8. Measured spectral response for the sensing and reference areas varying the incidence angle.

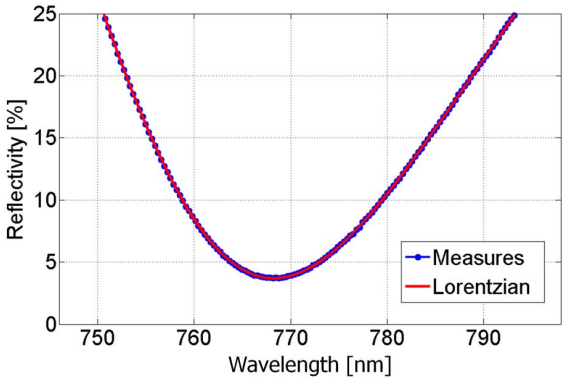

Fig. 9. Fitting of the reference resonance peak for a given angle of incidence with a Lorentzian function.

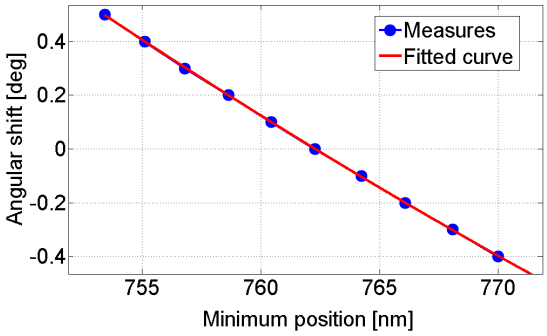

Fig. 10. Relationship between the spectral position of the reference resonance and the angular shift due to misalignments in launching the input beam.

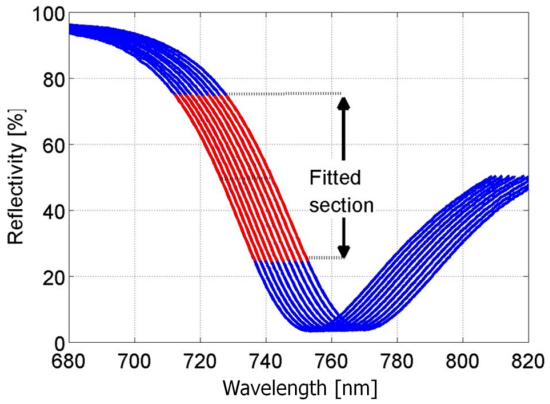

Fig. 11. Identification of the region around the 50% of sensor spectral dynamics used for the more accurate resonance peak location procedure.

the reference and analyte resonance position with accuracy in the order of the picometer.

However, common spectrometers have a resolution that is in the order of some hundreds of picometer; hence, to increase the accuracy in locating the spectral response minimum, the points within ∼20% of this value have been fitted using a Lorentzian function.

An example of the results is shown in Fig. 9 for the reference resonance, and shows an excellent overlap between the measured points and the analytical function.

Through this fitting applied to the all the curves in Fig. 8 corresponding to the resonances of the reference refractive index material, the relation between the wavelength of the resonance peak and the angular shift can be derived, as shown in Fig. 10.

As anticipated, the experiments confirm that the relationship between the position of the minimum in the spectral response and the angular misalignment, at least for small drift, is almost linear.

To assess the compensation procedure an intentional angular misalignment of $+0.180°$ has been introduced. This corresponds to a shift in the reference resonance wavelength from 764.226 to 760.759 nm, and in the analyte resonance wavelength from 636.124 to 634.917 nm, as determined from the fitting procedure around the respective position of their minima in the sensor spectral response, with an apparent refractive index variation of the analyte of $6.68{\cdot}10^{-4}$ RIU. From the plot in Fig. 10, it is found that the shift in the reference resonance corresponds to an angular shift of 0.185°. Using the new angle, the error in the determination of the analyte refractive index reduces to $3.54{\cdot}10^{-5}$ RIU. The improvement is more than one order of magnitude, but, being larger than the target value, which was in the order of some units in 10^{-6} RIU, it also highlights that the estimation in the resonance peak position is not accurate enough.

Hence, the possibility to fit other portions of the sensor spectral response has been investigated, with the objective to improve the compensation accuracy through an improvement of the resonance peak location.

Particularly, interesting is the region ∼50% of the spectral dynamics (Fig. 11) because it corresponds to the largest value of the first derivative, hence to the maximum sensitivity to the curve spectral position.

Upon determination of a new compensating curve similar to that shown in Fig. 10, using this peak alternative identification procedure, and applying the angular correction to the evaluation of the analyte refractive index, the error reduces to $5.06{\cdot}10^{-6}$ RIU, which is in line with the expected compensation effectiveness.

The same procedure has been applied with other angles, always obtaining an improvement of the same order of magnitude. Moreover, the measurement procedure has turned out to be reproducible and stable, since the measurements have been

repeated several times, in different days, and no appreciable difference in the result has been found.

V. Conclusion

The working principle of an optical sensor for chemicals with compensation of the environmental induced perturbations has been presented. Typical application is in the monitoring of the concentration of specific chemicals, such as pollutants or pesticides, in water solutions over a long time. Furthermore, the devised sensor configuration is particularly well suited for being implemented in POF, thus taking advantage of an all-fiber, but low cost and setup.

A model to study the effectiveness of the compensation approach has been developed and experimentally validated. The tests have been focused mainly on the evaluation of the impact of angular misalignments and the results shown that using the proposed compensation an improvement of more than an order of magnitude in the uncertainty is achievable, provided that the location of the peaks of the resonances is accurate within a few picometers. This is not directly achievable with common low-cost spectrometers and thus suitable spectral response fitting procedures must be applied to increase the instrument resolution.

References

[1] O. S. Wolfbeis, "Fiber-optic chemical sensors and biosensors," *Anal. Chem.*, vol. 85, no. 2, pp. 4269–4283, 2008.

[2] B. Lee, S. Roh, and J. Park, "Current status of micro- and nano-structured optical fiber sensors," *Opt. Fiber Technol.*, vol. 15, no. 3, pp. 209–221, 2009.

[3] J. Homola, S. S. Yee, and G. Gauglitz, "Surface plasmon resonance sensors: Review," *Sens. Actuators B, Chem.*, vol. 54, no. 1, pp. 3–15, 1999.

[4] A. K. Sharma, R. Jha, and B. D. Gupta, "Fiber-optic sensors based on surface plasmon resonance: A comprehensive review," *IEEE Sensors J.*, vol. 7, no. 8, pp. 1118–1129, Aug. 2007.

[5] J. Homola, "Optical fiber sensor based on surface plasmon excitation," *Sens. Actuators B, Chem.*, vol. 29, nos. 1–3, pp. 401–405, 1995.

[6] E. Fontana, H. D. Dulman, D. E. Doggett, and R. H. Pantell, "Surface plasmon resonance on a single mode optical fiber," *IEEE Trans. Instrum. Meas.*, vol. 47, no. 1, pp. 168–173, Feb. 1998.

[7] C. Pulido and O. Esteban, "Multiple fluorescence sensing with side-pumped tapered polymer fiber," *Sens. Actuators B, Chem.*, vol. 157, no. 2, pp. 560–564, 2011.

[8] G. Perrone and A. Vallan, "A low-cost optical sensor for noncontact vibration measurements," *IEEE Trans. Instrum. Meas.*, vol. 58, no. 5, pp. 1650–1656, May 2009.

[9] E. Angelini, S. Grassini, A. Neri, M. Parvis, and G. Perrone, "Plastic optic fiber sensor for cumulative measurements," in *Proc. IEEE IMTC*, 2009, pp. 1666–1670.

[10] R. Slavík, J. Homolaa, J. Btyroky, and E. Bryndab, "Novel spectral fiber optic sensor based on surface plasmon resonance," *Sens. Actuators B, Chem.*, vol. 74, nos. 1–3, pp. 106–111, 2001.

[11] C. Fallauto, G. Perrone, and A. Vallan, "Differential surface plasmon resonance sensor for the detection of chemicals and biochemicals," *Key Eng. Mater.*, vol. 543, pp. 310–313, Mar. 2013.

[12] C. Fallauto, Y. Liu, G. Perrone, and A. Vallan, "A differential optical sensor for long-term monitoring of chemicals," in *Proc. IEEE Int. IMTC*, May 2013, pp. 620–623.

[13] H. Q. Zhang, S. Boussaad, and N. J. Tao, "High-performance differential surface plasmon resonance sensor using quadrant cell photodetector," *Rev. Sci. Instrum.*, vol. 74, pp. 150–153, Jan. 2003.

[14] J. Ptasinski, L. Pang, P. C. Sun, B. Slutsky, and Y. Fainman, "Differential detection for nanoplasmonic resonance sensors," *IEEE Sensors J.*, vol. 12, no. 2, pp. 384–388, Feb. 2012.

[15] L. C. Oliveira, C. da Silva Moreira, C. Thirstrup, E. U. K. Melcher, A. M. N. Lima, and H. Neff, "A surface plasmon resonance biochip that operates both in the angular and wavelength interrogation modes," *IEEE Trans. Instrum. Meas.*, vol. 62, no. 5, pp. 1223–1232, May 2013.

[16] (2013). *Refractive Index of Materials* [Online]. Available: http://www.luxpop.com

[17] (2013). *Refractive Index of Materials* [Online]. Available: http://www.refractiveindex.info

[18] (2008). *Temperature Coefficient of Refractive Index* [Online]. Available: http://www.schott.com

[19] P. Schiebener, J. Straub, J. M. H. Levelt Sengers, and J. S. Gallagher, "Refractive index of water and steam as function of wavelength, temperature and density," *J. Phys. Chem. Ref. Data*, vol. 19, no. 3, pp. 677–717, 1990.

[20] X. Wang, Y. Tang, C. Zhou, and B. Liao, "Theoretical investigation of a dual-channel optical fibre surface plasmon resonance hydrogen sensor based on wavelength modulation," *Meas. Sci. Technol.* vol. 24, 2013.

Carmelo Fallauto received the M.S. degree in electronic engineering from Politecnico di Torino, Torino, Italy, in 2011, where he is currently pursuing the Ph.D. degree in metrology. His thesis is on the design and realization of a system for the remote control of a wireless sensor network.

His current research interests include fiber sensors for chemical and physical quantities.

Yu Liu received the M.S. degree in telecommunications engineering from Politecnico di Torino, Torino, Italy, in 2012, where she is currently pursuing the Ph.D. degree in electronics.

Her current research interests include the applications of optical fibers to sensors and lasers.

Guido Perrone (M'97) received the Ph.D. degree in electromagnetics from Politecnico di Torino, Torino, Italy, where he is currently a Professor of microwaves and optical fibers and components.

His current research interests include fiber optic sensors and high power fiber lasers.

Dr. Perrone is a member of the IEEE/MTTS, the IEEE/Photonics Society, and the Optical Society of America.

Alberto Vallan (SM'12) received the M.S. degree in electronic engineering from Politecnico di Torino, Torino, Italy, in 1996, and the Ph.D. degree in electronic instrumentation from the University of Brescia, Brescia, Italy, in 2000.

He is currently an Assistant Professor of electronic measurements with the Department of Electronics and Telecommunications, Politecnico di Torino. His current research interests include digital signal processing and development and characterization of sensors and measuring instruments for industrial applications.

Dr. Vallan is a Senior Member of the IEEE/I2MTC Society.